European Review for Medical and Pharmacological Sciences 2013; 17: 2916-2922

Detection of prostate cancer related copy number variations with SNP genotyping array

Y. WANG, X. YAO[1], S.-N. LI[2], A.-L. SUO[2], T. TIAN[2], Z.-P. RUAN[2], H. GUO[2], Y. YAO[2]

Department of Endocrinology, The First Affiliated Hospital of Xi'an Jiaotong University, Xi'an, Shaanxi, China
[1]Department of General Surgery, The Center Hospital of Xi'an, Xi'an, Shaanxi, China
[2]Department of Oncology, The First Affiliated Hospital of Xi'an Jiaotong University, Xi'an, Shaanxi, China

Abstract. – AIM: Prostate cancer is characterized by the accumulation of multiple copy number variants (CNVs) across the genome. We aim to identify potential prostate cancer related CNVs.

MATERIALS AND METHODS: Whole-genome SNP genotyping data of 18 prostate cancer patients was downloaded from the GEO (Gene Expression Omnibus) database. PennCNV was used to detect CNVs. All genes and miRNAs affected by CNVs were annotated. We also identified biological processes where these genes over-represented to capture the characteristics of prostate cancer.

RESULTS: Dominance of deletions was identified in all subjects. A total of 131 genes and 2 miRNAs which were affected by CNVs supported by at least two samples were detected. Over-representations of biological processes related with immune or inflammation response and cell cycle were identified. Two miRNAs, hsa-miR-1302 and hsa-miR-548j, were affected by CNVs and their target genes were reported to be related with prostate cancer according to the Mendelian Inheritance in Man database.

CONCLUSIONS: We identified genes known to be affected by prostate cancer associated CNVs in previous studies; we also identified new genes and miRNAs not reported as interesting. The discoveries in this study may advance the knowledge of the prostate cancer pathogenesis.

Key Words:
Prostate cancer, CNV, Pathway, miRNA.

Introduction

Prostate cancer is one of the main contributors to total disability-adjusted life-years worldwide[1]. It is the first leading cause of cancer-related death in men in UK[2] and internationally it is the sixth[3]. Prostate cancer is particularly prevalent in developed countries and the incidence is increasing in developing world[3]. Prostate cancer is characterized by the accumulation of multiple copy number variants (CNVs) across the genome. Identification of CNVs associated with pathological characteristics may help in identifying key genes in the progression of prostate cancer and further represent new prognostic markers and therapeutic targets for the clinical management of the disease. Compared with single-nucleotide polymorphisms (SNPs), CNVs represent genomic copy number deletions or duplications which may help explain some of the heritability that is not accounted by SNPs.

Accumulating evidence has demonstrated that certain CNVs are associated with a low to moderate cancer risk in prostate cancer[4]. Prior studies of CNVs detection using comparative genomic hybridization (CGH) arrays and SNP arrays have identified many CNVs on different chromosome arms across the genome, such as 2q, 3q, 5q, 6q, 7q, 8p, 8q, 10q, 13q, 16q, 17q, 18q, 21q and Xq[5-8]. These identifications have advanced our knowledge of prostate cancer, and highlighted the importance of some genes involved in prostate carcinogenesis, such as *PTEN*[6]. Compared with CGH arrays, detection of CNVs using whole-genome SNP genotyping arrays is more sensitive owing to its improved resolution and genome coverage.

Here with a public high-resolution genome-wide SNP genotyping data downloaded from the Gene Expression Omnibus (GEO) database, we detected potential prostate cancer associated CNVs. Specifically, we identified individual genes affected by CNVs in each tumor and the pathways in which these genes involved. We also identified biological processes where these genes over-represented to capture the clinicopathological characteristics of prostate cancer. Moreover, we also identified miRNAs affected by CNVs to explore the potential molecular mechanism underlie the pathogenesis of the disease.

Corresponding Author: Yu Yao, MD; e-mail: 13572101611@163.com

Materials and Methods

SNP Array Data

Prostate cancer SNP array dataset GSE29569[9] was downloaded from the GEO (http://www.ncbi.nlm.nih.gov/geo) database. Genotype data of prostate cancer and adjacent normal tissues from 18 prostate cancer patients (Table I) were included. The data set was based on the platform GPL6801: Affymetrix Genome-Wide Human SNP 6.0 Array.

CNV Detection

The PennCNV[10] software was used for CNV detection. PennCNV is a hidden Markov model (HMM) based approach for kilobase-resolution detection of CNVs using high-density SNP genotyping data. Briefly, CNVs were detected as follows: first, raw signal intensity values were normalized and experiment-wide normalized signal intensity on the A and B alleles for each SNP was generated; second, the log R Ratio (LRR) value and B Allele Frequency (BAF) of each SNP were calculated; third, CNVs were then detected using a first-order HMM model which assumes that the hidden copy number state of each SNP depends only on the copy number state of the most preceding SNP. The types of CNVs in all samples were calculated.

Identification of Chromosome Bands with Significantly Frequent CNVs

The expected number of CNVs in a chromosome band (UCSC) was calculated by the total number of CNVs and the CNV rate. Tests of significance for each band were performed by assuming a Poisson distribution.

Annotation

We retrieved segmental whole genome annotation information from the UCSC Genome Browser[11] for CNVs which were detected in at least two samples. Genes in CNVs were annotated through the Kyoto Encyclopedia of Genes and Genomes (KEGG) pathway analysis[12] and Gene Ontology (GO) analysis[13]. In addition, miRNAs in CNVs were annotated according to the miRbase release 19 (http://www.mirbase.org/ftp.shtml). Target genes of the miRNAs were predicted using Targetscan (Version 6.2)[14], miRDB (http://mirdb.org/miRDB/), miRanda[15], miRWalk[16], and PicTar[17]. Information of the Online Mendelian Inheritance in Man (OMIM) database was used to check whether the target genes were reported to be related with prostate cancer before. Whether the proteins encoded by the genes in CNVs interact with each other was also investigated based on the NCBI database (http://ftp.ncbi.nlm.nih.gov/gene/GeneRIF/, 2013-2-25).

Results

Genotype data of tumor and adjacent normal tissues from 18 prostate cancer patients (Table I) were used for CNV detection. According to the PennCNV analysis results (Table II), all subjects were detected with more deletions than duplications.

The genome-wide distribution of CNVs among the 18 prostate cancer cases is illustrated in Figure 1. Our analysis identified frequent CNVs on chromosome arms 1q, 3q, 4q, 6q, 8p, 9q, 10q, 13q, 15q, 16q, 20p, 21q, and 22q ($p < 0.01$, Table III).

Annotation based on human reference sequence (NCBI Build 36.1, hg18) showed that a total of 131 genes and 2 miRNAs were involved in CNVs which were detected in at least two samples. Pathway analysis based on the KEGG database showed that 34 genes were mapped to 92 pathways. Two genes, *PTEN* and *RB1* are involved in the prostate cancer pathway (hsa05215). Interaction analysis revealed that the protein encoded by *CHEK2* directly interacts with the RB1 protein. *RB1* and *CHEK2* are both involved in the cell cycle pathway (hsa04110). Protein encoded by *FRK* directly interacts with the PTEN and RB1 protein. With respect to genetic information processing, *ERG* is involved in the transcriptional misregulation in cancers pathway (hsa05202) and *SNRPD3* is involved in the spliceosome pathway (hsa03040). Variants in these pathways may impact the regular transcription process. Moreover, *MRPL13* is involved in the ribosome pathway (hsa03010) and CNVs in this pathway may interrupt the normal translation process.

To further determine the biological involvement of these CNVs and potential enrichment of biologically relevant process, we conducted GO analysis and cataloged the GO terms over-represented among the 18 tumors (Table IV, Fisher's exact p-value < 0.1).

In addition, two miRNAs, hsa-miR-1302 and hsa-miR-548j were involved in the CNVs. Target gene prediction results showed that their target genes were related with prostate cancer accord-

Table I. Detail information of the samples.

ID	Type	GSM	Description
P107	Normal	GSM732031	P107-N normal prostate
	Tumor	GSM732027	P107-TL1 prostate tumor
	Tumor	GSM732030	P107-TM1 prostate tumor
P123	Normal	GSM775363	P123-N normal prostate
	Tumor	GSM775361	P123-TL1 prostate tumor
SH12	Normal	GSM732036	SH12-N normal prostate
	Tumor	GSM732032	SH12-T1 prostate tumor
	Tumor	GSM732033	SH12-T2 prostate tumor
SH14	Normal	GSM732053	SH14-N normal prostate
	Tumor	GSM732043	SH14-T1 prostate tumor
	Tumor	GSM732048	SH14-T2 prostate tumor
SH17	Normal	GSM732064	SH17-N normal prostate
	Tumor	GSM732058	SH17-T1 prostate tumor
	Tumor	GSM732063	SH17-T2 prostate tumor
WX11	Normal	GSM731953	WX11-N normal prostate
	Tumor	GSM731951	WX11-TL1 prostate tumor
	Tumor	GSM731952	WX11-TL2 prostate tumor
WX12	Normal	GSM731956	WX12-N normal prostate
	Tumor	GSM731954	WX12-TL1 prostate tumor
	Tumor	GSM731955	WX12-TL2 prostate tumor
WX1	Normal	GSM731944	WX1-N normal prostate
	Tumor	GSM731942	WX1-TR1 prostate tumor
	Tumor	GSM731943	WX1-TR2 prostate tumor
WX21	Normal	GSM731959	WX21-N normal prostate
	Tumor	GSM731957	WX21-TL1 prostate tumor
	Tumor	GSM731958	WX21-TR1 prostate tumor
WX33	Normal	GSM731963	WX33-N normal prostate
	Tumor	GSM731960	WX33-TL1 prostate tumor
	Tumor	GSM731961	WX33-TL2 prostate tumor
	Tumor	GSM731962	WX33-TR1 prostate tumor
WX39	Normal	GSM731966	WX39-N normal prostate
	Tumor	GSM731965	WX39-TM1 prostate tumor
	Tumor	GSM731964	WX39-TR1 prostate tumor
WX47	Normal	GSM731969	WX47-N normal prostate
	Tumor	GSM731967	WX47-TL1 prostate tumor
WX68	Normal	GSM775357	WX68-N normal prostate
	Tumor	GSM775355	WX68-TL1 prostate tumor
WX73	Normal	GSM731972	WX73-N normal prostate
	Tumor	GSM731970	WX73-TL1 prostate tumor
	Tumor	GSM731971	WX73-TL2 prostate tumor
WX76	Normal	GSM731975	WX76-N normal prostate
	Tumor	GSM731973	WX76-TL1 prostate tumor
	Tumor	GSM731974	WX76-TL2 prostate tumor
WX8	Normal	GSM731947	WX8-N normal prostate
	Tumor	GSM731945	WX8-TL1 prostate tumor
	Tumor	GSM731946	WX8-TR1 prostate tumor
WX92	Normal	GSM731984	WX92-N normal prostate
	Tumor	GSM731976	WX92-TL1 prostate tumor
	Tumor	GSM731977	WX92-TL2 prostate tumor
	Tumor	GSM731979	WX92-TM1 prostate tumor
WX9	Normal	GSM731950	WX9-N normal prostate
	Tumor	GSM731948	WX9-TL1 prostate tumor
	Tumor	GSM731949	WX9-TR1 prostate tumor

Table II. Statistical information of the Copy Number Variants (CNVs) in all subjects.

Sample	cn=0	cn=1	cn=3	cn=4
P107	8	190	36	26
P123	21	140	28	13
SH12	25	83	67	28
SH14	47	80	28	21
SH17	56	579	31	9
WX1	18	32	18	7
WX11	21	37	10	8
WX12	25	97	15	11
WX21	13	341	27	26
WX33	17	215	172	22
WX39	41	76	30	15
WX47	9	239	20	7
WX68	21	263	44	8
WX73	19	80	6	14
WX76	8	96	77	18
WX8	19	100	27	9
WX9	11	320	102	64
WX92	19	108	9	15

Note: cn: copy number.

ing to the OMIM database. For example, *PDS5B* was predicted to be the target gene of these two miRNAs and it was reported in the OMIM database. Other four target genes of hsa-miR-548j, *CLU*, *STEAP2*, *KLF6*, and *STEAP4* were also reported to be related with prostate cancer.

Discussion

In this study, we screened out CNVs and genes involved in CNVs to infer the possible pathogenesis mechanisms of prostate cancer based on SNP genotyping arrays. The PennCNV software was used for CNV detection. As a HMM based approach, PennCNV considers SNP allelic ratio distribution as well as other factors, in addition to signal intensity alone, to infer CNV calls for individual genotyped samples[10].

Dominance of deletions was identified in all patients. Deletion of functional regions may result in abnormal proteins, contributing to the progression of prostate cancer. Previous CNV stud-

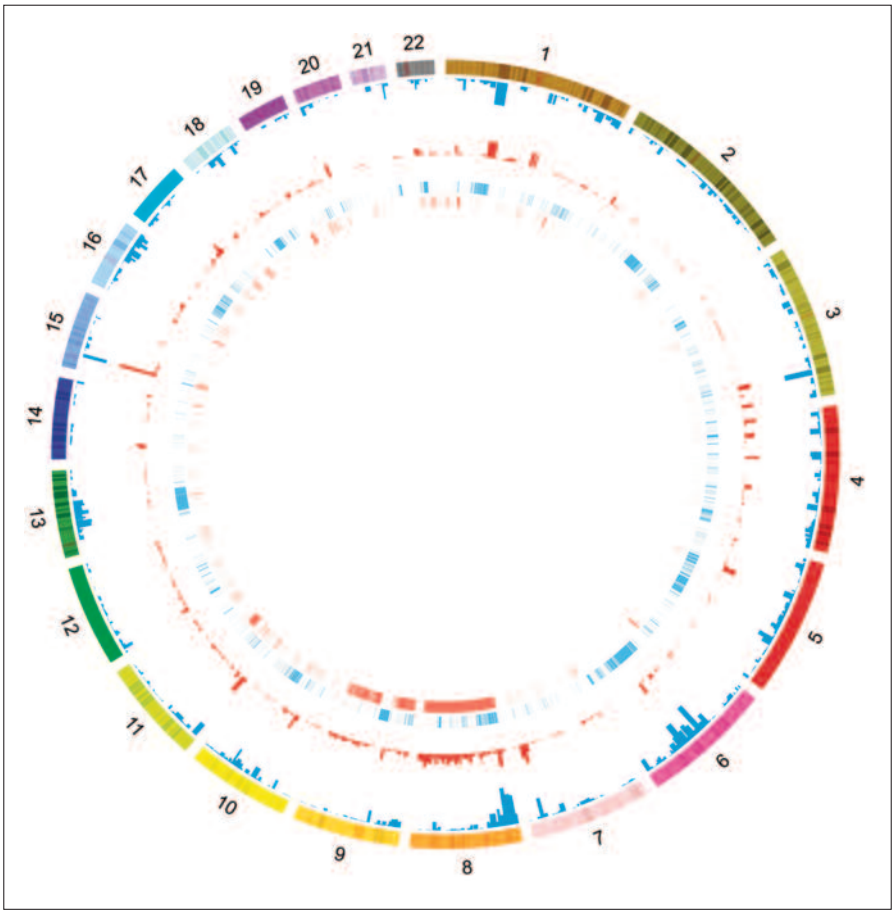

Figure 1. The genome-wide distribution of copy number variants (CNVs) among the 18 prostate cancer patients. The inner red bands display the range of duplications and the blue bands represent the range of deletions. The outer red histograms display the number of duplications while the blue histograms display the number of deletions.

Table III. Chromosome bands with frequent CNVs.

Chromosome	Start	End	Deletions	Duplications	Band	*p*-value
chr15	18400000	23300000	46	43	q11.2	1.84E-08
chr8	39500000	39900000	8	13	p11.22	5.01E-08
chr8	38500000	39500000	11	16	p11.23	3.18E-07
chr8	2200000	6200000	55	4	p23.2	1.27E-06
chr8	6200000	12700000	58	19	p23.1	7.28E-06
chr8	12700000	19100000	71	3	p22	1.06E-05
chr7	137300000	142800000	38	22	q34	3.32E-05
chr21	38600000	41400000	30	2	q22.2	1.26E-04
chr10	89600000	92900000	33	0	q23.31	3.35E-04
chr3	161200000	169200000	53	14	q26.1	3.80E-04
chr8	23400000	27400000	33	4	p21.2	4.74E-04
chr6	75900000	83900000	60	5	q14.1	5.28E-04
chr1	149600000	153300000	19	15	q21.3	6.04E-04
chr15	74400000	76100000	10	9	q24.3	7.83E-04
chr8	0	2200000	19	3	p23.3	1.00E-03
chr22	21800000	24300000	19	5	q11.23	1.04E-03
chr9	42400000	46700000	23	13	p11.2	1.10E-03
chr6	99900000	104800000	26	14	q16.3	1.10E-03
chr4	66300000	70400000	18	16	q13.2	1.32E-03
chr16	80500000	82700000	20	0	q23.3	2.30E-03
chr6	83900000	84700000	10	0	q14.2	3.69E-03
chr6	113900000	117100000	24	0	q22.1	4.95E-03
chr13	46200000	48900000	19	2	q14.2	5.12E-03
chr13	44300000	45900000	14	0	q14.12	6.58E-03
chr20	0	5000000	18	15	p13	6.77E-03
chr1	142400000	148000000	19	16	q21.1	8.95E-03

ies of prostate cancer have reported numerous chromosome regions[5,18]. Here we also identified similar results for a majority of previously reported chromosome arms, such as 1q, 3q, 4q, 6q, 8p, 9q, 10q, 13q, 15q, 16q, 21q, and 22q. For the genes in the CNVs, both *PTEN* and *RB1* are involved in the prostate cancer pathway (hsa05215). *PTEN* at 10q23 loss has also been identified in previous CNV studies[19,20]. Interaction analysis revealed that the protein encoded by *CHEK2* directly interacts with the RB1 protein. Both *RB1* and *CHEK2* are involved in the cell cycle pathway (hsa04110), abnormity of which may result in the malignant proliferation of cancer cells. Protein encoded by *FRK* directly interacts with both PTEN and RB1 protein. FRK protein is a nuclear protein and it may play important roles during G1 and S phase of the cell cycle and suppress cell growth. Deletion of this gene may also interrupt the regular cell cycle, resulting malignant cancer cells. Moreover, genes involved in genetic information processing were also identified, including *ERG*, *SNRPD3* and *MRPL13*, implicating the interruption of the normal transcription and translation process in prostate cancer. According to the literature review, no report of the association with *SNRPD3*, *MRPL13* and prostate cancer has been proposed before.

GO analysis identified over-representations of biological processes related with immune or inflammation response (Table IV), suggesting the involvement of the immune systems in prostate cancer. In addition, over-representations of biological processes related with cell cycle were also identified, such as negative regulation of cell aging, negative regulation of cell proliferation, and mitotic cell cycle G1/S transition checkpoint.

We also detected two miRNAs, hsa-miR-1302 and hsa-miR-548j, in the CNVs. No previous report has proposed the relationship between these two miRNAs and prostate cancer. However, target gene prediction analysis based on the OMIM database revealed that their target genes were re-

Table IV. Biological processes over-represented in genes affected by CNVs in each tumor.

Gene ontology biological process	Tumors affected (%)
T-helper 1 type immune response	8 (44.44)
Regulation of interleukin-10 secretion	8 (44.44)
Humoral immune response mediated by circulating immunoglobulin	8 (44.44)
Synapse maturation	8 (44.44)
Olfactory receptor activity	8 (44.44)
Peptide antigen binding	8 (44.44)
Immunoglobulin production involved in immunoglobulin mediated immune response	8 (44.44)
Regulation of interleukin-4 production	8 (44.44)
MHC class II protein complex	8 (44.44)
Defense response to bacterium	8 (44.44)
Extracellular region	8 (44.44)
Positive regulation of insulin secretion involved in cellular response to glucose stimulus	7 (38.89)
Negative regulation of cell aging	7 (38.89)
Negative regulation of cell proliferation	7 (38.89)
Clathrin-coated endocytic vesicle membrane	7 (38.89)
Transport vesicle membrane	7 (38.89)
Mitotic cell cycle G1/S transition checkpoint	7 (38.89)
G-protein coupled receptor activity	7 (38.89)
Plasma membrane	7 (38.89)
Keratinization	7 (38.89)
Phosphatidylinositol-3,4,5-trisphosphate 3-phosphatase activity	7 (38.89)
Regulation of centromere complex assembly	7 (38.89)
Trans-Golgi network membrane	7 (38.89)
Protein tetramerization	7 (38.89)

lated with prostate cancer. Among the target genes, *PDS5B* was predicted to be the target gene of both miRNAs. Protein encoded by *PDS5B* interacts with the conserved protein complex termed cohesion and it is a negative regulator of cell proliferation. Most epithelial cells of adult prostate gland are in a state of proliferative quiescence. This growth restriction effect is regulated by androgens through increasing the expression of PDS5B[21]. Therefore, deletion of the two miRNAs we detected here may interrupt the regular androgen's growth restriction effect on normal prostate epithelial cells.

Conclusions

Using a genome-wide SNP array data and PennCNV analysis, we identified genes known to be affected by prostate cancer associated CNVs in previous studies; we also identified new genes and miRNAs not reported as interesting. The discoveries in this study may advance the knowledge of the prostate cancer pathogenesis.

Acknowledgements

This study was supported by the Science and Technology Research Foundation of Shannxi Province , P.R. China (No.2013K12-03-12).

Conflict of Interest

The Authors declare that there are no conflicts of interest.

References

1) Soerjomataram I, Lortet-Tieulent J, Parkin DM, Ferlay J, Mathers C, Forman D, Bray F. Global burden of cancer in 2008: a systematic analysis of disability-adjusted life-years in 12 world regions. Lancet 2012; 380: 1840-1850.
2) Siegel R, Ward E, Brawley O, Jemal A. Cancer statistics, 2011: the impact of eliminating socioeconomic and racial disparities on premature cancer deaths. CA Cancer J Clin 2011; 61: 212-236.
3) Baade PD, Youlden DR, Krnjacki LJ. International epidemiology of prostate cancer: geographical distribution and secular trends. Mol Nutr Food Res 2009; 53: 171-184.

4) Liu W, Sun J, Li G, Zhu Y, Zhang S, Kim ST, Wiklund F, Wiley K, Isaacs SD, Stattin P, Xu J, Duggan D, Carpten JD, Isaacs WB, Gronberg H, Zheng SL, Chang BL. Association of a germ-line copy number variation at 2p24.3 and risk for aggressive prostate cancer. Cancer Res 2009; 69: 2176-2179.

5) Sun J, Liu W, Adams TS, Sun J, Li X, Turner AR, Chang B, Kim JW, Zheng SL, Isaacs WB, Xu J. DNA copy number alterations in prostate cancers: a combined analysis of published CGH studies. Prostate 2007; 67: 692-700.

6) Ishkanian AS, Malloff CA, Ho J, Meng A, Albert M, Syed A, van der Kwast T, Milosevic M, Yoshimoto M, Squire JA, Lam WL, Bristow RG. High-resolution array CGH identifies novel regions of genomic alteration in intermediate-risk prostate cancer. Prostate 2009; 69: 1091-1100.

7) Liu W, Chang B, Sauvageot J, Dimitrov L, Gielzak M, Li T, Yan G, Sun J, Sun J, Adams TS, Turner AR, Kim JW, Meyers DA, Zheng SL, Isaacs WB, Xu J. Comprehensive assessment of DNA copy number alterations in human prostate cancers using Affymetrix 100K SNP mapping array. Genes Chromosomes Canc 2006; 45: 1018-1032.

8) Perner S, Demichelis F, Beroukhim R, Schmidt FH, Mosquera JM, Setlur S, Tchinda J, Tomlins SA, Hofer MD, Pienta KG, Kuefer R, Vessella R, Sun XW, Meyerson M, Lee C, Sellers WR, Chinnaiyan AM, Rubin MA. TMPRSS2:ERG fusion-associated deletions provide insight into the heterogeneity of prostate cancer. Cancer Res 2006; 66: 8337-8341.

9) Boyd LK, Mao X, Xue L, Lin D, Chaplin T, Kudahetti SC, Stankiewicz E, Yu Y, Beltran L, Shaw G, Hines J, Oliver RT, Berney DM, Young BD, Lu YJ. High-resolution genome-wide copy-number analysis suggests a monoclonal origin of multifocal prostate cancer. Genes Chromosomes Canc 2012; 51: 579-589.

10) Wang K, Li M, Hadley D, Liu R, Glessner J, Grant SF, Hakonarson H, Bucan M. PennCNV: an integrated hidden Markov model designed for high-resolution copy number variation detection in whole-genome SNP genotyping data. Genome Res 2007; 17: 1665-1674.

11) Kuhn RM, Karolchik D, Zweig AS, Trumbower H, Thomas DJ, Thakkapallayil A, Sugnet CW, Stanke M, Smith KE, Siepel A, Rosenbloom KR, Rhead B, Raney BJ, Pohl A, Pedersen JS, Hsu F, Hinrichs AS, Harte RA, Diekhans M, Clawson H, Bejerano G, Barber GP, Baertsch R, Haussler D, Kent WJ. The UCSC genome browser database: update 2007. Nucleic Acids Res 2007; 35: D668-673.

12) Kanehisa M, Goto S, Sato Y, Furumichi M, Tanabe M. KEGG for integration and interpretation of large-scale molecular data sets. Nucleic Acids Res 2012; 40: D109-114.

13) Ashburner M, Ball CA, Blake JA, Botstein D, Butler H, Cherry JM, Davis AP, Dolinski K, Dwight SS, Eppig JT, Harris MA, Hill DP, Issel-Tarver L, Kasarskis A, Lewis S, Matese JC, Richardson JE, Ringwald M, Rubin GM, Sherlock G. Gene ontology: tool for the unification of biology. The Gene Ontology Consortium. Nat Genet 2000; 25: 25-29.

14) Lewis BP, Burge CB, Bartel DP. Conserved seed pairing, often flanked by adenosines, indicates that thousands of human genes are microRNA targets. Cell 2005; 120: 15-20.

15) Betel D, Wilson M, Gabow A, Marks DS, Sander C. The microRNA.org resource: targets and expression. Nucleic Acids Res 2008; 36: D149-153.

16) Dweep H, Sticht C, Pandey P, Gretz N. miRWalk--database: prediction of possible miRNA binding sites by "walking" the genes of three genomes. J Biomed Inform 2011; 44: 839-847.

17) Krek A, Grun D, Poy MN, Wolf R, Rosenberg L, Epstein EJ, MacMenamin P, da Piedade I, Gunsalus KC, Stoffel M, Rajewsky N. Combinatorial microRNA target predictions. Nat Genet 2005; 37: 495-500.

18) Torring N, Borre M, Sorensen KD, Andersen CL, Wiuf C, Orntoft TF. Genome-wide analysis of allelic imbalance in prostate cancer using the Affymetrix 50K SNP mapping array. Br J Cancer 2007; 96: 499-506.

19) Jenkins RB, Qian J, Lieber MM, Bostwick DG. Detection of c-myc oncogene amplification and chromosomal anomalies in metastatic prostatic carcinoma by fluorescence in situ hybridization. Cancer Res 1997; 57: 524-531.

20) Cheng I, Levin AM, Tai YC, Plummer S, Chen GK, Neslund-Dudas C, Casey G, Rybicki BA, Witte JS. Copy number alterations in prostate tumors and disease aggressiveness. Genes Chromosomes Cancer 2012; 51: 66-76.

21) Maffini MV, Geck P, Powell CE, Sonnenschein C, Soto AM. Mechanism of androgen action on cell proliferation: AS3 protein as a mediator of proliferative arrest in the rat prostate. Endocrinology 2002; 143: 2708-2714.